PHYSICAL REVIEW B VOLUME 48, NUMBER 4 15 JULY 1993-II

Oxygen 1s x-ray absorption of tetravalent titanium oxides: A comparison with single-particle calculations

F. M. F. de Groot,* J. Faber, J. J. M. Michiels, M. T. Czyżyk,† M. Abbate, and J. C. Fuggle‡
Spectroscopy of Solids and Surfaces, University of Nijmegen, Toernooiveld, 6525 ED Nijmegen, The Netherlands
(Received 5 November 1992; revised manuscript received 25 January 1993)

The oxygen 1s x-ray-absorption spectra of $SrTiO_3$ and TiO_2, in both the rutile and anatase crystal structure, are analyzed using the oxygen p-projected density of states of ground-state band-structure calculations. Good agreement is found and it is concluded that multielectron effects, transition matrix elements, and the core-hole potential present only small, largely undetectable, influences on the spectral shape. From the site- and symmetry-projected density of states the rutile peaks could be assigned to the 3d band (4–8 eV), antibonding oxygen 2p states (10–18 eV), and the titanium 4sp band (20–25 eV). For anatase the titanium 4sp band is shifted to lower energy by about 5 eV, which can be related to the lower density of anatase. From differences in the crystal structure it is argued that the core-hole potential is considerably more effective in perovskite $SrTiO_3$ than in both TiO_2 crystal structures. This is in accordance with the experimental findings.

I. INTRODUCTION

The aim of this study is to clarify the interpretation of the spectral shape of the oxygen 1s x-ray-absorption spectra of tetravalent titanium oxides. The oxides in which the formal valency of titanium is 4+ are characterized by a band gap placed in between the oxygen 2p valence band and the titanium 3d conduction band, making these compounds nonmetallic. The empty 3d band is a fortunate feature for single-particle models to describe the electronic structure accurately. For the comparison to x-ray-absorption spectra it is particularly important that all two-electron integrals are ineffective. In the ground state, with only completely filled or empty bands this is the case. The final state of oxygen 1s x-ray absorption contains a core hole in the oxygen 1s level and at the edge the excited electron is positioned in the 3d band and from dipole selection rules must bear oxygen p character. All (multipole effects from) two-electron integrals $\langle 1s,np|1/r|1s,np\rangle$ for the oxygen core hole can safely be neglected. The final state contains only one electron in the 3d band, thus also the $\langle 3d,3d|1/r|3d,3d\rangle$ integrals are not effective. This is in clear contrast with titanium 2p x-ray absorption on the same compounds. The $\langle 2p,3d|1/r|2p,3d\rangle$ integrals are large and strongly couple the core hole to the 3d states, the result being excitoniclike $2p^5 3d^3$ final states.[1–3] For the analysis of titanium 2p x-ray-absorption spectra, single-particle calculational schemes are not capable of reproducing the spectral shape. In this paper we would like to investigate the extent to which single-particle schemes are effective for the analysis of the oxygen 1s spectra.

A usual picture to visualize the electronic structure of a transition-metal monoxide is to describe the chemical bonding mainly as a bonding between the metal 4sp states and the oxygen 2p states, forming a completely filled bonding combination, usually denoted as the oxygen 2p band, and a completely empty antibonding combination denoted as the metal 4s and 4p bands. The 3d states also form a chemical bonding to the oxygen 2p states which causes them to be antibonding in nature and additionally this bonding, taking place in a cubic crystalline surrounding of oxygen atoms, causes the 3d states to be split into the t_{2g} and e_g manifolds.

II. CALCULATIONS

This qualitative description of the electronic structure of transition-metal oxides can be worked out quantitatively in single-particle models describing the infinite solid with band-structure calculations formalized within the local-density approximation (LDA) of density-functional theory.[4,5] We have performed LDA calculations for TiO_2 rutile, anatase, and $SrTiO_3$ with the objective of comparing the oxygen 1s x-ray-absorption spectra with a set of equivalent calculations. The calculations are dedicated to the analysis of the unoccupied states and we have used basis sets, which yield accurate results up to about 25 eV above the Fermi level.

The calculations have been performed using the localized spherical wave (LSW) method. The LSW method has evolved out of the augmented spherical wave (ASW) method of Williams, Kübler, and Gelatt:[6] the idea of tight-binding muffin-tin orbitals suggested by Andersen and Jepsen[7] for the linearized-muffin-tin-orbital (LMTO) method, has been reformulated and implemented for the ASW method.[8] In order to describe accurately the unoccupied states over a wider energy range, the LSW method has been modified to include an extended basis set allowing two functions for each angular momentum on each site.[9–12]

In order to avoid problems related to overlap between the spheres it is necessary to include empty spheres at open positions in the crystal structures. In $SrTiO_3$ and anatase one empty sphere position is included and for rutile two different empty spheres are included. Table I

TABLE I. Structural information. The point-group and unit-cell parameters are taken from Ref. 13. The atomic radii as used in the LSW calculations are given for all different atoms (in Å) for their respective Wyckoff positions.

Compound	$SrTiO_3$	TiO_2 (rutile)	TiO_2 (anatase)
Point-group unit-cell parameters	P_{m3m} $a=3.905$	$P4_2/mnm$ $a=4.594$ $c=2.959$ $u=0.305$	$I4_1/amd$ $a=3.784$ $c=9.515$ $u=0.206$
	Radii and Wyckoff positions		
titanium	0.92 1*b*	0.70 2*a*	0.76 4*a*
oxygen	1.03 1*a*	1.00 4*f*	1.00 8*e*
strontium	1.57 3*c*		
empty spheres	0.50 12*j*	0.65 4*d* 0.54 4*g*	0.68 8*e*

contains the structural information as used in the calculations. It has been checked that with different sets of atomic radii, chosen within reasonable limits, the results are equivalent for the accuracy needed. The atomic radii are necessary in the calculations to divide the space. They have no well-defined physical meaning and, for example, the amount of charge residing on each atom is dependent on the radii. Table II gives the states included in the calculations. The self-consistent potential is calculated for the valence states. The density of states is calculated with an extended basis set in order to obtain accurate results up to about 25 eV above the Fermi level. Figure 1 gives the density of states (DOS) of (a) $SrTiO_3$, (b) TiO_2, rutile, and (c) TiO_2, anatase. The figures contain the total DOS (bottom) and the DOS per site for the constituents oxygen, titanium, and strontium.

Comparison with other LDA calculations

In Table III we compare some electronic structure parameters as have been found from a series of recent band-structure calculations. We compare (i) the band gap, (ii) the width of the valence band, (iii) the width of the t_{2g} band, (iv) the width of the e_g band, and (v) the energy difference between the average energies of the t_{2g} and e_g bands, which we define as the effective crystal-field splitting (CFS). These values can be determined from the dispersion curves published and they can be inferred from cases where only density-of-states curves are given. We compare the band gap, the width of the valence band, and the CFS to experimental values in Table IV.

TABLE II. The states used in the calculations. The self-consistent potential is calculated with all valence states. To obtain the density of states accurate up to about 25 eV above E_F the extended basis set is used. An asterisk denotes that in the case of rutile and anatase the titanium 4*d*, 5*s*, and 5*p* states have been included in the extended basis set.

Element	Core states	Valence states	Extended basis
Sr	1*s*2*s*2*p*3*s*3*p*3*d*4*s*4*p*	5*s*5*p*4*d*	4*f*
Ti	1*s*2*s*2*p*3*s*3*p*	4*s*4*p*3*d*	4*f*, (4*d*5*s*5*p**)
O	1*s*	2*s*2*p*3*d*	3*s*3*p*
empty	none	1*s*	

For rutile a large series of calculations are available and it can be checked in Table III that the calculations of Refs. 14–18 are consistent with the present calculation. The variations in the five parameters as given in Table III are generally within 0.3 eV. The band gap is found to be 2.0 eV in Refs. 14–16 and 2.5 eV in Ref. 17 and in our result, in comparison with the experimental value of 3.06 eV as determined from optical absorption, which recently was confirmed by resonant hyper Raman.[25] This underestimation of the band gap is a well-known feature of LDA calculations and is a result of the inadequacy to describe the actual electron additional and electron removal spectra directly by using the density of states of a single-particle calculation. That the experimental band gap is found in the calculation of Munnix and Schmeits[18] is not surprising as they use a semiempirical potential.

III. EXPERIMENT

The x-ray-absorption spectra have been measured at BESSY, using the SX700(I) monochromator. The spectra are recorded in total electron yield mode. The samples, rutile and anatase natural minerals and a commercial $SrTiO_3$ single crystal, were scraped with a ruby file, at UHV conditions to ensure surface cleanliness. The rutile spectrum has been published earlier.[29] Equivalent spectra have been published by van der Laan and co-workers[30] and by Brydson and co-workers.[21,22]

IV. RESULTS AND INTERPRETATION

Figure 2 gives the comparison of the projected density of states with the oxygen 1*s* x-ray-absorption results for (a) $SrTiO_3$, (b) rutile TiO_2, and (c) anatase TiO_2. The spectra have been aligned at the position of the first peak. The oxygen *p*-projected DOS has been broadened with a Gaussian function of 0.3 eV half-width at half maximum. The broadening has been deliberately chosen too small in order to show the underlying structure.

For rutile the first two peaks are reproduced and if the broadening is optimized a close to perfect fit of the experiment is obtained. The splitting between the t_{2g} and the e_g peak is equal in experiment (2.7 eV) and theory (2.8 eV).[27] We note that in the multiple scattering calculations of Refs. 21 and 22 a splitting of about 4 eV is found, which we tend to attribute to inaccuracies in their (non-self-consistent) potential. The structure between 10 and 22 eV is reproduced in the calculations and we conclude that the density of states as obtained from a ground-state calculation gives an accurate description of the oxygen 1*s* x-ray-absorption spectral shape. This implies that (i) there are no detectable many-electron effects, (ii) the core-hole potential does not have a large influence on the spectral shape, and (iii) the energy variation of the transition matrix elements can be neglected. Vice versa this implies that the oxygen 1*s* x-ray-absorption spectral shape gives a direct picture of the oxygen *p*-projected density of states.

The site and symmetry projection of the density of states offers the possibility of analyzing the respective structures in terms of particular bands. The t_{2g} and e_g bands are dominated by titanium 3*d* states. The structure between 10 and 22 eV has been assigned to the titanium 4*s* and 4*p* bands or more precisely to the antibonding combinations of oxygen 2*p* and titanium 4*sp* states.[29] The present calculations modify this assignment: the titanium *s*-projected DOS (not shown) has a sharp maximum around 22 eV, which places the titanium 4*s* band in between 20 and 23 eV and similarly the titanium 4*p* band in between 21 and 27 eV. This leaves us with the question about the nature of the states in between 10 and 20 eV. These states are dominated by oxygen *p* character and they are best assigned as antibonding combinations of direct oxygen-oxygen interactions.

For anatase we also find good agreement between the first two peaks in the calculation and in experiment.

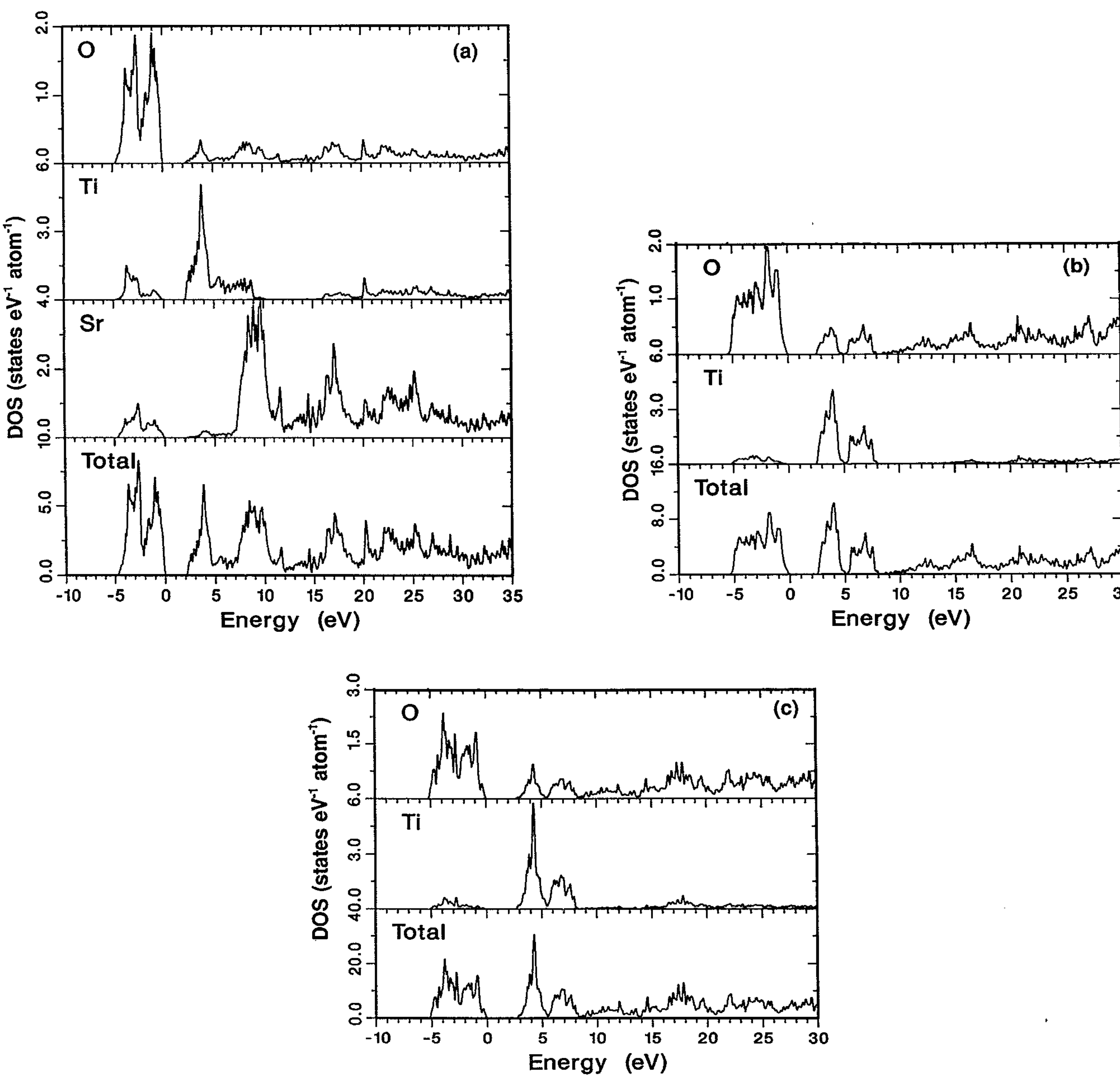

FIG. 1. The site-projected density of states of (a) $SrTiO_3$, (b) rutile TiO_2, and (c) anatase TiO_2. In the plots as given the density of states has been broadened by 0.1 eV full width at half maximum. The total DOS, with units "states 1 eV cell," has been given at the bottom. For the oxygen, titanium, and strontium the DOS has been given per site.

TABLE III. Comparison of electronic structure parameters as determined by a series of recent band-structure calculations. Abbreviations: LMTO (linear muffin-tin orbitals), APW (augmented plane waves), LSW (linearized spherical waves), and CFS (crystal-field splitting). All values in eV.

Compound	Band gap	Width valence band	Width T_{2g} band	Width E_g band	CFS	Method	Ref.
Rutile	2.0	5.7	2.9	3.3	2.5	Pseudopotential	14 and 15
Rutile	2.0	5.4	2.6	3.3	2.7	LMTO	16
Rutile	2.6	6.5	2.8	3.5	3.5	LMTO	17
Rutile	3.1	5.5	2.2	3.2	2.5	APW	18
Rutile	3.1	8.5	2.4	1.3	4.2	LMTO	19
Rutile	10	7				Hartree-Fock	20
Rutile			4	4	7	Multiple scattering	21 and 22
Rutile	2.5	5.4	2.8	3.1	2.8	LSW	this work
Anatase	2.7	5.2	2.8	3.0	2.9	LSW	this work
$SrTiO_3$	6.3	2.7	2.0	3.0	2.7	APW	23
$SrTiO_3$	2.9	5.5	2.3	3.6	2.5	LMTO	24
$SrTiO_3$	2.1	5.0	2.6	4.3	3.2	LSW	this work

There is some mismatch in the structured second peak which has too much intensity in the calculation and also the calculated splitting is slightly larger (2.9 versus 2.6). Compared to rutile the main differences are the structure in between 10 and 20 eV. In the case of anatase a clear two-peaked structure is observed with peak maxima at about 12 and 18 eV. This two-peaked structure is reproduced in the calculations with some overestimation of the intensity of the 18-eV peak and a slightly shifted 12-eV peak maximum. Analysis of the site- and symmetry-projected DOS (not given) reveals that the titanium 4s band is positioned in between 16 and 18 eV, and similarly the titanium 4p band is positioned in between 17 and 20 eV, which is exactly at the position of the second peak in experiment. Thus we can assign the 18-eV peak to the titanium 4sp band, while the 12-eV peak is assigned again as antibonding oxygen 2p states. A possible cause for the large intensity of the 18-eV peak is the size of radius around oxygen, which apparently overestimates the oxygen character in titanium-dominated states. This will be solved if the transition matrix elements are taken into account quantitatively.

TABLE IV. Comparison of the calculated values of the band gap and the crystal-field splitting with experimentally determined values. All values in eV.

Compound	Band gap	Crystal-field splitting	Method	Ref.
Rutile	2.5	2.8	Theory	this work
	3.06		Res. Raman	25
		2.6	O 1s XAS	this work
		2.7	O 1s EELS	21 and 22
		1.8	Ti 2p XAS	2 and 27
Anatase	2.7	2.9	Theory	this work
		2.6	O 1s XAS	this work
		2.6	O 1s EELS	21 and 22
$SrTiO_3$	2.1	3.2	Theory	this work
	3.18		Res. Raman	26
		2.8	O 1s XAS	this work
		2.9	O 1s EELS	21 and 22
		1.5	Ti 2p XAS	27 and 28

For $SrTiO_3$ a different spectral shape is observed. The sharp t_{2g} peak is followed by a small e_g peak in experiment and this e_g peak is blurred by the next structure in the calculations. From the site-projected DOS in Fig. 1 it can be seen that the e_g peak is spread out from 4.5 to 9 eV while at about 7.5 eV the strontium-related peak sets in. This strontium-related peak has its peak positions at 8, 9.5, and 11.5 eV in the calculation while the experiment gives 8.5, 10.5, and 12 eV. Thus while the overall shape of this peak is reproduced in detail it is shifted downwards in the calculation. Thus it appears that the e_g peak is smaller in width in experiment and the strontium-related structure is shifted by about 0.5 eV. A possible reason for the sharper e_g peak is the core-hole potential, which will be more visible for $SrTiO_3$ because the e_g band is broad and flat (see Fig. 1) compared to the more round shaped and narrower peak for rutile and anatase (see also the next section).[32] A second reason is the shift in the strontium peaks tends to blur a separate structure of the e_g peak. The next peak at about 16 eV appears at about 18 eV in the calculations while the structure in between 21 and 23 eV has an identical position in the calculation. The symmetry projection (not given, see Ref. 31) shows that the 18-eV peak is dominated by strontium p character while the structure in between 21 and 23 eV can be assigned to the titanium 4sp band.

Relation to crystal structures

The crystal structures of rutile, anatase, and perovskite ($SrTiO_3$) are all markedly different and here we will try to correlate this with the observed spectral shapes. The distorted octahedra share four edges in anatase and two in rutile. In the rutile structure they form chains along the [001] axes and in isostructural VO_2 the vanadium atoms form twins along these [001] axes, which share their 3*d* electrons to form an overall singlet state.[33,34] TiO_2 does not contain any electrons in the 3*d* band, hence no energy can be gained by their (effective) interaction. The oxygen-titanium network in perovskite is best viewed as a simple cubic structure of titanium atoms with an oxygen atom halfway between each titanium pair. Hence only titanium-oxygen bonds exist and no direct titanium-titanium interactions are possible. In fact at room temperature the structure is perfectly cubic with all Ti-O-Ti bondings 180°.[23]

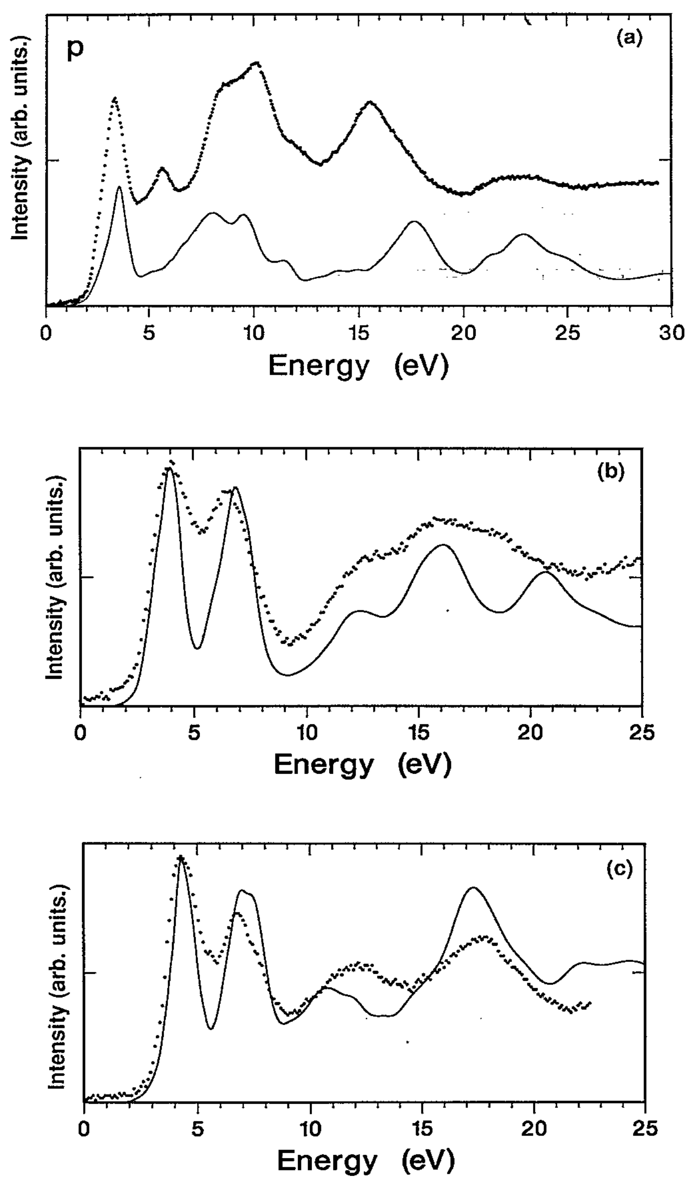

FIG. 2. Comparison of the oxygen 1*s* x-ray-absorption spectra (dotted) with the oxygen *p*-projected density of states (solid line) for (a) $SrTiO_3$, (b) rutile TiO_2, and (c) anatase TiO_2. The spectra have been normalized arbitrarily. The oxygen *p*-projected DOS has been broadened with 0.3 eV half-width at half maximum.

The difference in titanium-oxygen bonds in perovskite versus anatase and rutile has a different effect on the shape of the 3*d* band. Perovskite can be considered as the prototype for a tight-binding description of the TiO_6^{8-} cluster. The t_{2g} states are π bonding and the e_g states form σ bonds, hence the empty and antibonding 3*d* band is split into a t_{2g} band at a higher energy than the e_g band. Because of the stronger σ interaction the dispersion in the e_g band is much larger. This picture is reproduced in the band-structure calculation and can best be observed in the titanium-projected DOS in Fig. 1(a), where the sharp narrow t_{2g} states are followed by the dispersed e_g states. In both rutile and anatase the octahedra are distorted, which has the consequences of (i) causing an additional splitting of the t_{2g} and e_g bands and (ii) allowing cation-cation as well as anion-anion interactions to be more prominent thereby making the tight-binding description less precise. The net effect will be that the t_{2g} and e_g bands are less pure π versus σ bonded and will tend to appear more alike in width. This can be seen in Figs. 1(b) and 1(c). This difference between perovskite and rutile/anatase reappears in the oxygen 2*p* valence band, which for perovskite clearly shows bonding and nonbonding subbands with titanium character more prominent in the bonding subband [Fig. 1(a)]. The distorted octahedra and particularly the more prominent oxygen-oxygen interactions largely blur the distinction between bonding and nonbonding and the titanium character is spread evenly over the valence band for both rutile and anatase [Figs. 1(b) and 1(c)].

This difference in structure has consequences for the effectiveness of the core-hole potential in perovskite versus rutile/anatase. In perovskite the e_g band is broadened over about 5 eV by dispersion, while in the case of rutile/anatase the broadening is less, but more importantly it is mainly caused by the tetragonal distortion of the octahedra, which gives rise to a splitting of the d_{z^2} and the $d_{x^2-y^2}$ orbitals. The core-hole potential tends to localize the electron in the excited state and hence it counteracts dispersional broadening. A splitting between d_{z^2} and the $d_{x^2-y^2}$ states cannot be removed by a core-hole potential and the core-hole potential is less effective in narrowing the e_g band in rutile and anatase. Because of the particular shape of the density of states, a narrowing is also more visible in perovskite. This can lead to the observations that the core-hole potential is apparently absent in rutile and anatase, while for perovskite it creates an additional sharp peak at the bottom of the e_g band which is not existing in the broadened density of states.

A remarkable difference between rutile and anatase is the spectral structure in between 10 and 25 eV. As discussed, the 12-eV peak in anatase and the 13- and 17-eV peaks in rutile can be assigned as antibonding oxygen states, while the titanium 4*sp* band is related to the 18-eV peak in anatase and the 22-eV peak in rutile. These states are at such energies that they can safely be considered as itinerant and hence the interactions causing their energy positions should scale with the volume per formula unit. Although anatase has shorter mean titanium-oxygen distances (by 0.5%), its volume is 34.1 Å^3 versus 31.2 Å^3 for rutile. Thus the anatase crystal has an 8% less dense structure and smaller effective interactions of the titanium 4*sp* states. Hence they are less antibonding and their position is at lower energy. A similar argument can be used for the antibonding oxygen states.

V. CONCLUDING REMARKS

For the comparison of the *p*-projected DOS with oxygen 1*s* x-ray-absorption detailed agreement has been found for rutile and anatase. This leads to the conclusion that many-electron effects, transition matrix elements, and the core-hole potential are all not effective. For $SrTiO_3$ the effect of the core-hole potential is more prominent for the e_g band, because of the large dispersional broadening of this band. For rutile and anatase the broadening is mainly caused by a tetragonal distortion of the octahedra, which cannot be counteracted by the core-hole potential.

The assignment of the bands has been modified from our earlier assignment.[29] The nature of the crystal-field-split 3*d* band is confirmed, but analysis of the site- and symmetry-projected density of states makes one readjust the assignment of the titanium 4*sp* band, which is found at about 22 eV in rutile and 18 eV in anatase. The structure just above the 3*d* band is not dominated by titanium 4*sp* character but instead by oxygen *p* character. Hence the related peaks in the spectrum have been assigned to antibonding oxygen 2*p* states, of course with a partial contribution of titanium 4*sp* states. For $SrTiO_3$ the first strontium-related bands overlap with the e_g band, which is confirmed by experiment.

The comparison of a series of different band-structure calculations shows that the recent self-consistent LMTO, pseudopotential, and LSW calculations give similar results for most electronic structure parameters. The earlier non-self-consistent calculations give, in general, better agreement for experimental parameters like the band gap, but this is a direct consequence of their semiempirical nature and/or adjustments made. The multiple-scattering calculations of Refs. 21 and 22 give less accurate results, which we relate to their non-self-consistent potential.

ACKNOWLEDGMENTS

This work was supported by the Dutch Foundation for Chemical Research (SON), the Dutch Organization for the Advancement of Research (NWO), and by the Dutch Foundation for Fundamental Research on Matter (FOM).

---

*Present address: Laboratoire pour l'Utilisation du Rayonnement Electromagnetique, Université Paris-Sud, Bâtiment 209D, F-91405 Orsay CEDEX, France.

†Present address: Department of Applied Physics, Rijksuniversiteit Groningen, Nijenborgh 4, 9747 AG Groningen, The Netherlands.

‡Deceased.

[1]B. T. Thole, C. van der Laan, and P. H. Butler, Chem. Phys. Lett. **149**, 295 (1984).

[2]F. M. F. de Groot, J. C. Fuggle, B. T. Thole, and G. A. Sawatzky, Phys. Rev. B **41**, 928 (1990).

[3]F. M. F. de Groot, J. C. Fuggle, B. T. Thole, and G. A. Sawatzky, Phys. Rev. B **42**, 5459 (1990).

[4]P. C. Hohenberg and W. Kohn, Phys. Rev. **136**, 864 (1964).

[5]W. Kohn and L. J. Sham, Phys. Rev. **140**, 1133 (1965).

[6]A. R. Williams, J. Kübler, and C. D. Gelatt, Jr., Phys. Rev. B **19**, 6094 (1979).

[7]O. K. Andersen and O. Jepsen, Phys. Rev. Lett. **53**, 2571 (1984); O. K. Andersen, O. Jepsen, and D. Glötzel, in *Highlights of Condensed Matter Theory*, edited by F. Bassani, F. Fumi, and M. Tosi (North-Holland, Amsterdam, 1985), pp. 59ff.

[8]F. Springelkamp, M. T. Czyżyk, and R. A. de Groot (unpublished); see also H. van Leuken, A. Lodder, M. T. Czyżyk, F. Springelkamp, and R. A. de Groot, Phys. Rev. B **41**, 5613 (1990).

[9]M. T. Czyżyk, R. A. de Groot, G. Dolba, P. Fornasini, A. Kisiel, F. Rocca, and E. Burattini, Phys. Rev. B **39**, 9831 (1989).

[10]M. T. Czyżyk and R. A. de Groot, in *Conference Proceedings of the 2nd European Conference on Progress in X-ray Synchrotron Radiation Research*, edited by A. Balerna, E. Bernieri, and S. Mobilio (SIF, Bologna, 1990), p. 47.

[11]M. Grioni, M. T. Czyżyk, F. M. F. de Groot, J. C. Fuggle, and B. E. Watts, Phys. Rev. B **39**, 4886 (1989).

[12]M. T. Czyżyk, R. Potze, and G. A. Sawatzky, Phys. Rev. B **46**, 3829 (1992).

[13]R. W. G. Wyckoff, *Crystal Structures II* (Interscience, New York, 1964).

[14]K. M. Glassford and J. R. Chelikowsky, Phys. Rev. B **46**, 1284 (1992).

[15]K. M. Glassford, J. Troullier, J. L. Martins, and J. R. Chelikowsky, Solid State Commun. **76**, 635 (1990).

[16]B. Poumellec, P. J. Durham, and G. Y. Guo, J. Phys. Condens. Matter **3**, 8195 (1991).

[17]N. I. Medvedeva, V. P. Zhukov, M. Y. Khodos, and V. A. Gubanov, Phys. Status Solidi B **160**, 517 (1990).

[18]S. Munnix and M. Schmeits, Phys. Rev. B **30**, 2202 (1984).

[19]M. A. Khan, A. Kotani, and J. C. Parlebas, J. Phys. Condens. Matter **3**, 1763 (1991).

[20]B. Silvi, N. Fourati, R. Nada, and C. R. A. Catlow, J. Phys. Chem. Solids **52**, 1005 (1991).

[21]R. Brydson, H. Sauer, W. Engel, and F. Hofer, J. Phys. Condens. Matter **4**, 3429 (1992).

[22]R. Brydson, H. Sauer, W. Engel, J. M. Thomas, E. Zeitler, N. Kosugi, and H. Kuroda, J. Phys. Condens. Matter **1**, 797 (1989).

[23]L. F. Mattheiss, Phys. Rev. B **6**, 4718 (1972).

[24]Y. N. Xu, W. Y. Ching, and R. H. French, Ferroelectrics **111**, 23 (1990).

[25]K. Watanabe, K. Inoue, and F. Minami, Phys. Rev. B **46**, 2024 (1992).

[26]K. Watanabe and K. Inoue, J. Phys. Soc. Jpn. **58**, 726 (1989).

[27]It is noted that the crystal-field splitting obtained from titani-

um 2p x-ray absorption refers to the final-state value as discussed in Refs. 2 and 3.
[28]F. M. F. de Groot, M. O. Figueiredo, M. J. Basto, M. Abbate, H. Petersen, and J. C. Fuggle, Phys. Chem. Min. **19**, 140 (1992).
[29]F. M. F. de Groot, M. Grioni, J. C. Fuggle, J. Ghijsen, G. A. Sawatzky, and H. Petersen, Phys. Rev. B **40**, 5715 (1989).
[30]G. van der Laan, Phys. Rev. B **41**, 12 366 (1990); G. van der Laan, C. S. Mythen, and H. A. Padmore, Europhys. Lett. **11**, 67 (1990).
[31]F. M. F. de Groot, Ph.D. thesis, University of Nijmegen, 1991.
[32]The effect of the core-hole potential is to increase the intensity at the bottom of the band, which is more directly visible for a relatively flat broadband. For model calculations we refer to J. F. van Acker, Ph.D. thesis, University of Nijmegen, 1990.
[33]J. Goodenough, J. Solid State Chem. **3**, 490 (1971).
[34]M. Abbate, F. M. F. de Groot, J. C. Fuggle, Y. J. Ma, C. T. Chem, F. Sette, A. Fujimori, Y. Ueda, and K. Kosuge, Phys. Rev. B **43**, 7263 (1991).